Reprinted for private circulation from
GEOPHYSICS
Vol. 37, No. 5, October, 1972

DOWNWARD CONTINUATION OF MOVEOUT-CORRECTED SEISMOGRAMS†

JON F. CLAERBOUT* AND STEPHEN M. DOHERTY*

Earlier work developed a method of migration of seismic data based on numerical solutions of partial differential equations. The method was designed for the geometry of a single source with a line of surface receivers. Here the method is extended to the geometry of stacked sections, or what is nearly the same thing, to the geometry where a source and receiver move together along the surface as in marine profiling. The basic idea simply stated is that the best receiver line for any reflector is just at (or above) the reflector. Data received at a surface line of receivers may be extrapolated by computer to data at a hypothetical receiver line at any depth. By considering migration before stacking over offset, it is found that certain ambiguities in velocity analysis may be avoided.

THE SIMPLEST CASE

For the sake of clarity we begin with the simplest case for which migration is a useful concept. Then realistic complications can be included in order of their practical importance. First, consider a two-dimensional model of the earth, y horizontal, z downward, in which the seismic velocity c is constant but the reflectors have arbitrary dips and curvatures. Here we neglect shear waves, although they can be treated by the method of Landers and Claerbout (1972). We also neglect multiples and energy spreading into the third dimension. Multiples will be treated in a later paper. Let there be sources and receivers uniformly spaced over the y axis at intervals of Δy. We can suppose that all of our shots are set off in unison. (Even if they are not we may synthesize it in a computer by adding seismograms together.) At some depth which is very great compared to Δy the semicircular wavefronts will combine together in the fashion of Huygens secondary sources to make a downgoing wave which is essentially a plane wave. In other words, at sufficient depth, point sources along the surface are indistinguishable from a surface line source. It turns out that in practice there are usually not enough shots and deep enough reflectors for the plane-wave approximation to be very good. Nevertheless, this is a useful starting point and we will return later to consider the fact that the downgoing wave is not a plane wave.

Considering the downgoing wave to be merely an impulsive plane wave simplifies the task of migration because we then may turn our attention entirely to the upgoing wave; since, according to the basic principle (Claerbout, 1971b)

† Paper presented at the 41st Annual International SEG Meeting, November 9, 1972, Houston, Texas. Manuscript received by the Editor November 19, 1971; revised manuscript received April 6, 1972.

* Stanford University, Stanford, California 94305.

© 1972 by the Society of Exploration Geophysicists. All rights reserved.

"reflectors exist at points in the earth where the first arrival of the downgoing wave is time coincident with an upgoing wave."

A useful departure from our earlier work is that we are now migrating data from many shotpoints at a time, whereas previously each shotpoint was migrated separately before summation. The major effort in migration is to take the observed upgoing wave at the surface and project it back downward. A frequency-domain technique for this downward projection is given in Claerbout (1970 and 1971b). Here we will give a time-domain method because it leads to our central topic of downward continuation of moveout-corrected seismograms.

We are basically interested in projecting upgoing waves back into the earth. As pointed out in earlier papers, great economy and stability can be achieved by specializing the wave equation, which is second order and has both upgoing and downgoing solutions, to a first-order equation with only upgoing solutions. The first step is to re-express the scalar wave equation in a coordinate frame which translates upward with the speed c. In such a moving coordinate frame, the upcoming waves will be Doppler shifted to lower frequencies and the downgoing waves will be Doppler shifted to higher frequencies. Then a low-pass filtering type of operation can separate up from downgoing waves.

We have the scalar wave equation

$$0 = \frac{\partial^2 P}{\partial y^2} + \frac{\partial^2 P}{\partial z^2} - \frac{1}{c^2}\frac{\partial^2 P}{\partial t^2}, \tag{1}$$

which we abbreviate as

$$0 = P_{yy} + P_{zz} - c^{-2}P_{tt}. \tag{2}$$

We have the transformation to a coordinate frame translating upward with velocity c

$$y' = y, \tag{3a}$$

$$z' = z + ct, \quad \text{and} \tag{3b}$$

$$t' = t, \tag{3c}$$

and we have the statement that the new coordinate frame contains the same wave disturbance as the old frame.

$$P(y, z, t) = P''(y', z', t'). \tag{4}$$

To express the wave equation (2) in terms of the translating coordinate system, we may use the chain rule for partial differentiation. Obviously, $P_y = P'_{y'}$ and

$$P_{yy} = P'_{y'y'}. \tag{5}$$

Also

$$P_z = P'_{y'}y'_z + P'_{z'}z'_z + P'_{t'}t'_z = P'_{z'},$$

so

$$P_{zz} = P'_{z'z'}. \tag{6}$$

The nontrivial differentiation is

$$P_t = P'_{y'}y'_t + P'_{z'}z'_t + P'_{t'}t'_t = cP'_{z'} + P'_{t'},$$

which on a second differentiation leads to

$$\begin{aligned} P_{tt} &= c(cP'_{z'z'} + P'_{t'z'}) + (cP'_{z't'} + P'_{t't'}) \\ &= c^2P'_{z'z'} + 2cP'_{t'z'} + P'_{t't'}. \end{aligned} \tag{7}$$

Now we insert (5), (6), and (7) into the scalar wave equation (2) and obtain the scalar wave equation in a translating frame,

$$0 = P'_{y'y'} - \frac{2}{c}P'_{t'z'} - c^{-2}P'_{t't'}. \tag{8}$$

The rightmost term $P''_{t't'}$ is proportional to the square of the Doppler-shifted frequency of a wave. Thus, dropping this term may be expected to have little effect on upgoing waves but a drastic effect on downgoing waves. In fact, dropping the last term of (8) has the desired effect of eliminating the downgoing waves altogether as can be seen by comparing these results to earlier work (Claerbout 1970, 1971a, b). Simply dropping the term does have the undesired effect of limiting velocity accuracy to about a percent at 15 degrees. Economical procedures for obtaining better than a percent accuracy at 45 degrees also may be found in the earlier work.

Dropping the last term from (8), we have

$$P'_{t'z'} = \frac{c}{2}P'_{y'y'}. \tag{9}$$

A computer algorithm for solving (9) is described in Claerbout and Johnson (1972) along with a more detailed discussion including accuracy, stability, and an air-wave example.

Knowing the form of the upcoming wave at the surface of the earth, we can use equation (9) to project the upgoing wave backwards in time and, thus, find the upgoing wave at greater and greater depths. Using the basic principle "reflectors exist at points in the earth where the first arrival of the downgoing wave is time coincident with an upgoing wave," and considering the downgoing wave to be a delta function at time $t = z/c$, we get for the earth structure $S(y, z)$

$$S(y, z) = \int P(y, z, t)\delta(t - z/c)dt, \tag{10}$$

where $P(y, z, t)$ is found by solving (9) for $P''(y', z', t')$ and then transforming $P''(y', z', t')$ to $P(y, z, t)$ with the inverse to equation (3).

MOVEOUT-CORRECTED SEISMOGRAMS

In the previous section we considered the data which would be recorded if all surface shots were set off at the same time. If the shots are not set off at the same time but data is recorded from each shot separately, simultaneous shooting can by synthesized in a computer by stacking the data. For each receiver all seismograms of the different shots are aligned by shot time and added together. In practice, moveout correction would be applied before stacking. This correction is intended to remove source-receiver geometrical effects. Since it was ignored in the previous section, the results were limited to very great depths where the correction is small.

Figure 1 defines a moveout corrected profile of seismic data. Great improvement in the partial differential-equation migration method results from the idea that an NMO profile and often a zero-offset section can be governed by a differential equation. Figure 1 illustrates how an NMO profile M may be constructed from an upcoming wave U by transcribing data values from the (y, t) plane to the (x, d) plane. This operation is actually a coordinate transformation of the data. Since the moveout-corrected profile is just the upcoming wave with coordinate axes deformed, it is not surprising that moveout-corrected profiles can be governed by an equation derived through a coordinate stretching transformation of the wave equation. The idea that there should be any advantage to using differential equations on synthetic things like moveout-corrected profiles (as compared to natural things like waves) arose out of the following observations: It is comparatively inefficient to let a wave packet propagate across a grid in a computer. It is much more efficient to describe a wave in a coordinate frame which moves along with the wave, as was done for the surface line source case in the beginning of this paper. In such a frame, things happen slowly and larger time increments may be used. There is a similar situation in a nearly layered medium where seismic arrivals (upcoming waves) fit nearly hyperbolic traveltime curves, and the object of a migration program is to deform the hyperboloids into lines which represent the layer-

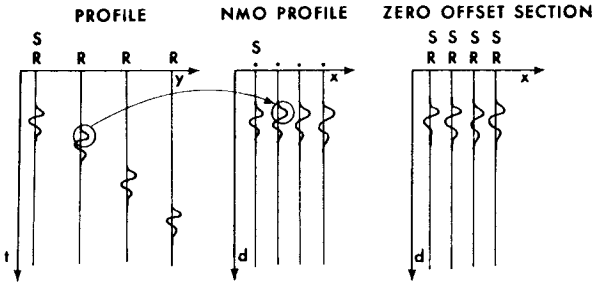

FIG. 1. Definition of profile and section. The left frame is indicative of observed upcoming waves recorded with one shot and a surface receiver line. This is called a *profile*. Data points are moved from this profile (y, t plane) to the central frame (x, d plane) under control of transformation equations like (13), with $z' = 0$. The central frame will be called an *NMO profile*. The third frame depicts upcoming waves recorded with a different shot receiver geometry. Each recording is made with the shot and receiver at the same location. This will be called a (zero-offset) *section*.

Although the methods of this paper assume the geometry of the *NMO profile*, they will often be applicable to data recorded as *sections*.

ing. A migration partial differential equation does a lot of work just moving energy around on a grid from one more or less predictable place to another. Considerable effort can be saved by doing moveout correction (including application of a time-variable velocity if necessary) to get energy in approximately the right place before requiring a differential equation to migrate the data to its final proper position. If reflecting layers are perfectly flat and level, migration makes no change to the moveout-corrected data. The greater the structural dips and curvatures, the greater will be the task for the migrating differential equation. Grid spacing can be chosen according to the maximum anticipated dip.

Although efficiency was the motivation in the search for a differential equation to control migration from moveout-corrected data, there are two concomitant benefits which are far more important than efficiency. First, the data from spatially separated shotpoints may be stacked before migration, thereby enhancing signal-to-noise ratio. Second, we often may dispense altogether with the line of surface receivers and migrate data recorded in the geometry, where shotpoint and receiver point move together across the earth's surface as in the simplest type of marine profiling.

By "downward continuation of moveout-corrected seismograms" we mean that beginning with moveout-corrected data observed at the surface, we will synthesize moveout-corrected seismograms corresponding to hypothetical receivers at successively increasing depths.

One reason for wanting the moveout-corrected data for buried receivers is that it is related, through geometry, to the upcoming wave which is needed to make a migrated profile. Another reason, which is really the same, relates to the nature of seismic diffraction. Figure 2 (after Hilterman, 1970) illustrates that a data section can be expected to resemble a cross-section through the reflector if the radius of curvature of the reflector is much greater than the distance from the reflector to the receiver. Otherwise, one has a buried focus or diffraction. (Technically, a diffraction is a limiting case where some radius of curvature of a structure goes to zero.) In other words, moveout-corrected data gives a better representation of a structure if the receivers are near the structure, than if they are far away. In fact, when the receivers are at the depth of the structure the buried focus problem disappears altogether. Diffractions from point scatterers also collapse to points when the receivers are at the same depth as the scatter. The method of migration proposed here is that as data are projected to successively greater depths, that part of the data corresponding to the receiver depth is set aside as belonging to the migrated data at that depth. Thus, various depths on the depth section are developed in succession as the moveout-corrected data are projected downward.

To be precise about the meaning of moveout-corrected data for buried receivers, we refer to Figure 3. Since the moveout-corrected profile M is created by a coordinate stretching of the upcoming wave U, we have

$$M(x, d, z') = U(y, t, z). \tag{11}$$

Observe the conceptual similarity of the relationship between $U(y, t, z)$ and $M(x, d, z')$ to the relationship between $P(y, z, t)$ and $P''(y', z', t')$. The fact that P and P'' are the same thing expressed in different coordinates is analogous to the fact that U and M are the same thing expressed in different coordinates. At the surface $z = 0$ we record the upcoming wave $U(y, t, 0)$, and using a presumed velocity (which need not be precisely correct), we transform axes to the NMO profile $M(x, d, 0)$. The downward (z) continuation of receivers of $U(y, t, z)$ with the wave equation will be equivalent to downward (z') continuation of $M(x, d, z')$ with an equation we are about to derive. Although these two different downward continuations would be expected to give the same results, i.e., one could transform from U to M or M to U at any depth, there are several reasons to prefer downward continuation with M: 1) profiles from various shotpoints may be summed before downward continuation, 2) a coarser grid mesh may be used, and 3) sections may be downward continued.

To obtain the differential equation for U, first we must define the coordinate transformation from (y, t, z) to (x, d, z') and then use the chain rule to compute the required partial derivatives. From Figure 3 by means of elementary geometry, one may deduce the transformation

$$y(x, d, z') = x \cdot (2 - z'/d), \tag{12a}$$

$$t(x, d, z') = (2d - z')(1 + x^2/d^2)^{1/2}/c, \tag{12b}$$

and

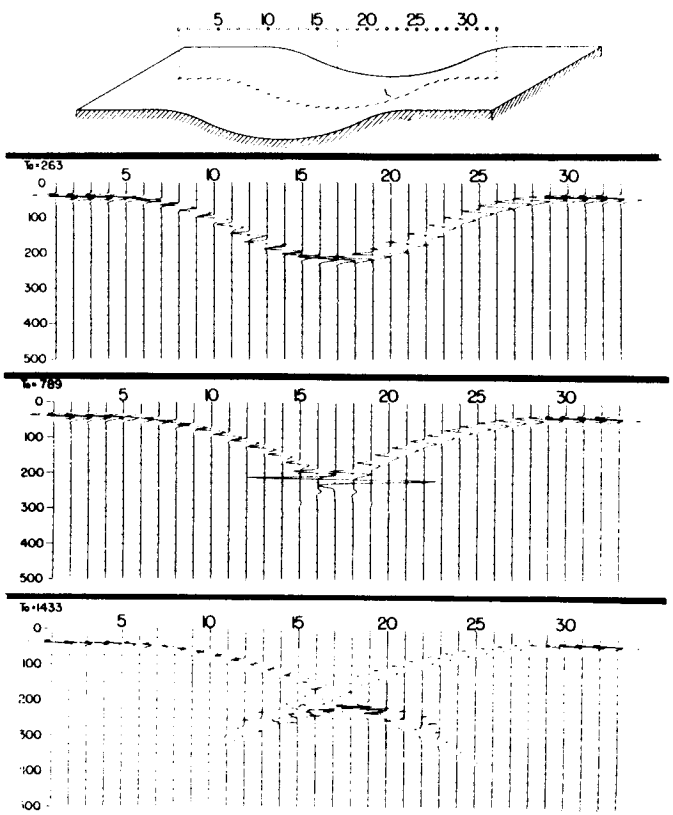

FIG. 2. (After Hilterman, 1970) Time sections recorded at various heights above a model. The top section ($T_0 = 263$) has shotpoint below the curvature axis, center section at the curvature axis, and bottom section above the curvature axis.

$$z(x, d, z') = z', \tag{12c}$$

and, by means of tedious algebra, the inverse transformation is found to be

$$d(y, t, z) = (z + (c^2t^2 - y^2)^{1/2})/2, \tag{13a}$$

$$x(y, t, z) = (y/2)(1 + z/(c^2t^2 - y^2)^{1/2}), \tag{13b}$$

and

$$z'(y, t, z) = z. \tag{13c}$$

In constant velocity material one could find an equation for M which is valid for all offsets x. The algebra would be overwhelming, so we make the simplifying practical assumption that $x/d \ll 1$. The authors were surprised to discover that even if offset terms like x/d or y/t are completely neglected one still obtains a result which is a big improvement over equation (9) of the introductory section. The reason is that even as offset goes to zero, the ratio of x to y remains important. Although (12) and (13) require a somewhat careful and detailed deduction, the zero offset relations are much easier and will be shown in detail. By

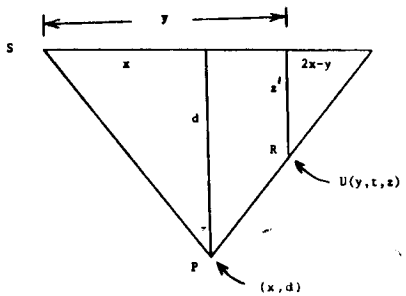

FIG. 3. Moveout correction geometry for buried receivers. There is a surface shot S and buried receiver R. The wave is assumed to reflect at the point P. The receiver R at (y, z') measures the upcoming wave $U(y, t, z)$. From the upcoming wave a moveout-corrected profile $M(x, d, z')$ is constructed by axis stretching according to the geometry of the raypath SPR.

similar right triangles, the ratio of x to d is the same as the ratio $2x-y$ to z'. Thus $x/d=(2x-y)/z'$ or

$$y(x, d, z') = x(2 - z'/d). \quad (14a)$$

The traveltime along SP will be d/c and along PR it will be $(d-z')/c$. Thus,

$$t(x, d, z') = (2d - z')/c. \quad (14b)$$

The zero offset limit of (12) is (14). Now for the inverse relations solve (14b) for d and use $z'(y, t, z)=z$,

$$d(y, t, z) = (ct + z)/2. \quad (15a)$$

Solve (14a) for x eliminating d with (15a) and using $z'=z$,

$$x = y/(2 - z/d)$$

and

$$x(y, t, z) = y/[2 - 2z/(ct + z)]. \quad (15b)$$

From the coordinate transformation (14) and its inverse (15), it will be an easy matter now to compute the partial derivatives required for the transformation of the upgoing wave equation. One derivative of particular interest, x_y, is computed from (15b) to be

$$x_y = 1/(2 - 2z/(ct + z)),$$

which in terms of the other variables is

$$x_y = 1/(2 - z'/d) = d/(2d - z'). \quad (16)$$

Computing all the partial derivatives at the zero offset limit and arranging into a matrix, we have

$$\begin{bmatrix} x_y & x_t & x_z \\ d_y & d_t & d_z \\ z'_y & z'_t & z'_z \end{bmatrix} = \begin{bmatrix} d/(2d - z') & 0 & 0 \\ 0 & c/2 & 1/2 \\ 0 & 0 & 1 \end{bmatrix}. \quad (17)$$

Now there are two possible ways to proceed. The simplest way is to use the chain rule and insert partial derivatives into the wave equation. Another way is to insert the partial derivatives into the upcoming-wave equation. Let us insert the partial derivatives into the wave equation (2).

$$U_{yy} + U_{zz} - c(y, z)^{-2}U_{tt} = 0. \quad (18)$$

We must be aware that (18) also has downgoing solutions which we will later eliminate by dropping a second order z' derivative. Recalling (11) that $U(y, t, z)=M(x, d, z')$, we compute the necessary terms for insertion into (18). Before insertion we simplify with the zeros in (17) and with the high-frequency approximation (gradients of waves are taken to be much greater than gradients of the coordinate transformation coefficients).

$$U_t = M_x x_t + M_d d_t = M_d d_t, \quad (19)$$

$$U_{tt} = M_{dd} d_t^2 \quad (20)$$

$$U_y = M_x x_y + M_d d_y = M_x x_y, \quad (21)$$

$$U_{yy} = M_{xx} x_y^2, \quad (22)$$

$$U_z = M_{z'} + M_x x_z + M_d d_z = M_{z'} + M_d d_z, \quad (23)$$

$$U_{zz} = M_{z'z'} + 2d_z M_{dz'} + M_{dd} d_z^2, \quad (24)$$

and

$$c(y, z) = c[y(x, d, z'), z(x, d, z')]. \quad (25)$$

Inserting (20), (22), (24), and (25) into (18) we obtain for the downward projection of the moveout-corrected data

$$M_{xx} x_y^2 + M_{z'z'} + 2M_{dz'} d_z + M_{dd}(d_z^2 - c^{-2} d_t^2) = 0, \quad (26)$$

which, utilizing (17) and the assumption that the true (wave-equation) velocity equals the constant stacking velocity (in d_t), simplifies to

$$M_{dz'} = -\left(\frac{d}{2d - z'}\right)^2 M_{xx} - M_{z'z'}. \quad (27)$$

The last term arises mainly because the wave equation we started from also has downgoing waves. The omission of this kind of term is discussed in the first section and in earlier papers. There is a formal similarity between (9) and (27), so the same computer algorithm may be used.

VARIABLE VELOCITY

The result of the last section, equation (27), is restricted to material of constant velocity. It will be useful in practice to generalize the result to space-variable velocity. First note that *the velocity $\tilde{c}$ in the wave equation (18) need not be the same as the velocity, say $\tilde{c}$, in the moveout-correction equations* (11) to (17). It can be shown that the wave equation is still valid at high frequencies ($\omega \gg |\nabla c|/c$) when the velocity $\tilde{c}$ is space variable, although the moveout-correction equations must be modified if the velocity $\tilde{c}$ is to be space variable. Thus, (26) is a valid equation for downward continuation in variable-velocity material for data stacked at a constant velocity c. The principal change to (27) resulting from space-variable velocity is that the M_{dd} term does not drop out. The difficulty which arises if $\tilde{c} \neq c$ is not in the differential equation (26) but in the fact that there may be destructive interference when stacking with the wrong velocity. Therefore we will recompute the partial-derivative matrix (17) for arbitrary depth dependence of stacking (moveout-correction) velocity. This will require some care. The matrix of (17) is really the Jacobian matrix of the transformation from (y, t, z) variables to (x, d, z') variables, that is:

$$\begin{bmatrix} dx \\ dd \\ dz' \end{bmatrix} = \begin{bmatrix} x_y & x_t & x_z \\ d_y & d_t & d_z \\ 0 & 0 & 1 \end{bmatrix} \begin{bmatrix} dy \\ dt \\ dz \end{bmatrix}. \quad (28)$$

The inverse transformation may be defined as

$$\begin{bmatrix} dy \\ dt \\ dz \end{bmatrix} = \begin{bmatrix} y_x & y_d & y_{z'} \\ t_x & t_d & t_{z'} \\ 0 & 0 & 1 \end{bmatrix} \begin{bmatrix} dx \\ dd \\ dz' \end{bmatrix}. \quad (29)$$

The statement that (29) is indeed inverse to (28) is

$$\begin{bmatrix} x_y & x_t & x_z \\ d_y & d_t & d_z \\ 0 & 0 & 1 \end{bmatrix} \begin{bmatrix} y_x & y_d & y_{z'} \\ t_x & t_d & t_{z'} \\ 0 & 0 & 1 \end{bmatrix} = \begin{bmatrix} 1 & 0 & 0 \\ 0 & 1 & 0 \\ 0 & 0 & 1 \end{bmatrix}. \quad (30)$$

Near the zero offset limit x and y tend to zero and are, therefore, independent of t, d, and z, so that $x_t = x_z = y_d = y_{z'} = 0$. Also, a small change in x or y has a second-order effect on traveltime so $t_x = d_y = 0$. Thus, at small enough offsets (30) reduces to

$$\begin{bmatrix} x_y & 0 & 0 \\ 0 & d_t & d_z \\ 0 & 0 & 1 \end{bmatrix} \begin{bmatrix} y_x & 0 & 0 \\ 0 & t_d & t_{z'} \\ 0 & 0 & 1 \end{bmatrix} = \begin{bmatrix} 1 & 0 & 0 \\ 0 & 1 & 0 \\ 0 & 0 & 1 \end{bmatrix}. \quad (31)$$

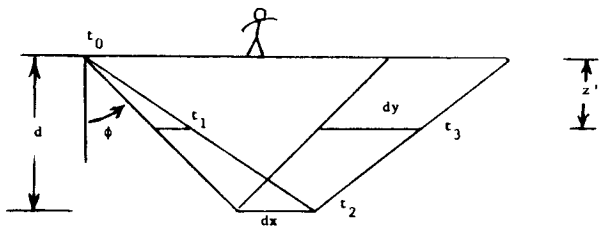

FIG. 4. Geometry for calculation of $(\partial x/\partial y)_t = 1/(\partial y/\partial x)_d$.

The interesting parts of (31) are

$$x_y = 1/y_z, \tag{32}$$

$$d_t t_d = 1, \tag{33}$$

and

$$d_t t_{z'} + d_z = 0. \tag{34}$$

To compute the partial derivative x_y, refer to Figure 4 which, for clarity, exaggerates the offset. For rays which are essentially vertical

$$dz = c\,dt. \tag{35}$$

We have Snell's law,

$$(\sin\phi)/c = \text{const} = p. \tag{36}$$

Tracing rays in time gives

$$x = \int_0^{t_2} c \sin\phi\, dt = p\int_0^{t_2} c^2 dt,$$

and using (35),

$$x = p\int_0^d c\,dz \tag{37}$$

and

$$y = p\int_0^{t_2} c^2 dt,$$

which, from Figure 4, may be written as

$$y = p\left(2\int_0^d c\,dz - \int_0^{z'} c\,dz\right). \tag{38}$$

It is convenient to use d and z' as superscripts to indicate integration in the same way we use them as subscripts to denote differentiation. Thus, we define

$$c^d = \int_0^d c(z)dz,\quad c^{z'} = \int_0^{z'} c(z)dz,$$

and use (37) to eliminate p from (38);

$$y = x(2c^d - c^{z'})/c^d. \tag{39}$$

Differentiating with respect to x holding d and z' constant, gives

$$y_x = (2c^d - c^{z'})/c^d. \tag{40}$$

Thus, using (32),

$$x_y = c^d/(2c^d - c^{z'}). \tag{41}$$

In the constant velocity limit (41) obviously reduces to (16).

The partial derivatives of traveltime t with respect to receiver depth and with respect to recording position are found in a similar manner. The traveltime dt through a layer of thickness dz is given by

$$dt = dz/c(z)\cos\phi,$$

where ϕ is the angle from the ray to the vertical. Replacing $1/\cos\phi$ by $1+\sin^2\phi/2$, we have

$$dt = \left(\frac{1}{c(z)} + \frac{\sin^2\phi}{2c(z)}\right)dz.$$

Using (36) and (37) to second order in x, we get

$$dt = \left(\frac{1}{c(z)} + \frac{x^2 c(z)}{2(c^d)^2}\right)dz.$$

Referring to Figure 4 we note that the traveltime is twice the time from 0 to d, less the time from 0 to z'. Thus,

$$t = 2\int_0^d \left[\frac{1}{c(z)} + \frac{x^2 c(z)}{2(c^d)^2}\right]dz - \int_0^{z'} \left[\frac{1}{c(z)} + \frac{x^2 c(z)}{2(c^d)^2}\right]dz.$$

This equation may be used to find the partial derivatives of traveltime to first order accuracy in x. However, in this section we are interested in finding the derivatives to zero order in x, so the terms proportional to x^2 may be omitted, giving

$$t = 2\int_0^d \frac{1}{c(z)}dz - \int_0^{z'} \frac{1}{c(z)}dz,$$

which we abbreviate as

$$t = 2(c^{-1})^d - (c^{-1})^{z'}. \tag{42}$$

Differentiating (42) with respect to d holding x and z' fixed, gives

$$t_d = +2/c(d), \tag{43}$$

where $c(d)$ is velocity $c(z)$ evaluated at $z=d$.

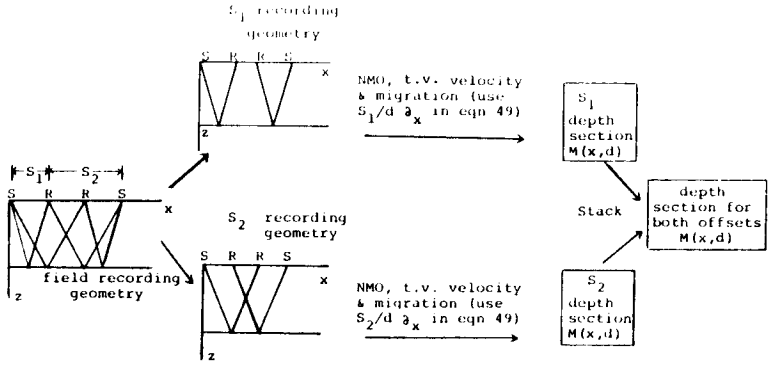

FIG. 5. Procedure for migrating data with several offsets. Field data are recorded using two receiver offsets, S_1 and S_2. The field data are separated into two sets: data recorded with offset S_1 and data recorded with offset S_2. Moveout corrections are done for both sets of data. Then the S_1 data are migrated with equation (49) with $(S_1/d)\partial_x$ substituted for $(x/d)\partial_x$, giving the S_1 depth section, $M(x,d)$. Next the S_2 data are migrated with equation (49) with $(S_2/d)\partial_x$ substituted for $(x/d)\partial_x$, giving the S_2 depth section, $M(x, d)$. Finally, the S_1 depth section and S_2 depth section are stacked to give the composite depth section.

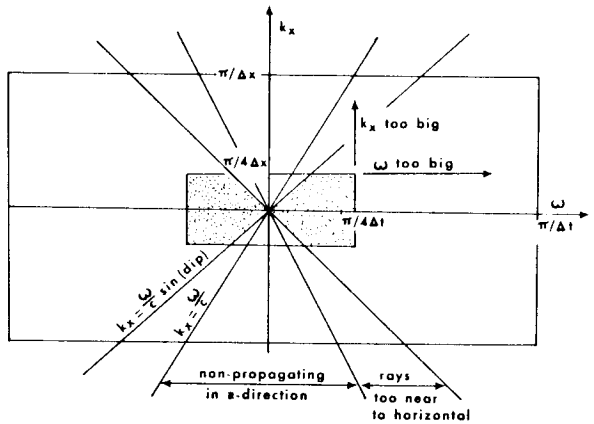

FIG. 6. The (ω, k) plane. Field data may be expected to have some energy everywhere in the (ω, k) plane. Only in the speckled region will our difference equations properly simulate the wave equation. Energy with $|k| > |\omega/c|$ does not represent free waves; it represents either surface waves or errors in data collection (often statics, random noise, or gain not smoothly variable from trace to trace). Such energy can mean nothing in a migration program, hence it should be rejected by filtering. This may be done by fan filtering (as in Treitel et al, 1967) or as was done here by means of numerical viscosity (Claerbout, 1970). Actually, for practical reasons one frequently may wish to reject rays outside a certain dip angle. This gives the larger fan filter reject region $|k| > |\omega/c \sin(\text{dip})|$. In fact our present implementation is inadequate for dips greater than about 45 degrees (Claerbout, 1971). Although information can be carried up to the folding frequency in both ω and k, in practice the use of operators of finite length narrows the useful bandwidth. As shown in Claerbout and Johnson (1972) the use of simple difference operators results in a practical bandwidth restriction to about a quarter of the folding frequency. This presents no problem in principle; data may be interpolated before processing, or more elaborate (i.e., longer) difference operators may be used. Finally, the figure was drawn with $\Delta x > c\Delta t$ because it represents the usual case in practice where extra points in time are more cheaply obtained than extra points in space.

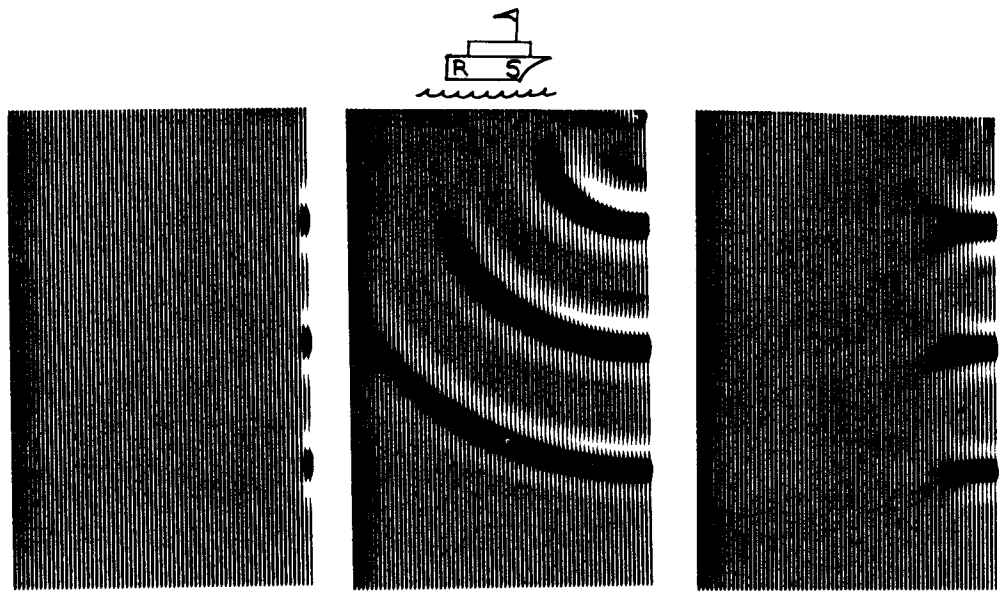

FIG. 7. The depth response to time-domain impulses and reconstruction of the impulses. The fact that the left frame is mostly blank depicts a situation in which no echo is received when a source and receiver move together in the horizontal direction until they reach the right-hand edge of the frame where the three blips indicate that there are three echoes at successively increasing times. With this as observed data, the logical conclusion is that the reflection structure of the earth is three concentric circles with centers on the right margin. The central frame shows the circles. (For economy the right edge of the frame is a plane of symmetry.) It will be noticed that the bottom of the circles is darker than the top. This is indicative of the 45-degree phase shift of bringing two-dimensional waves from a focus away from the focus. Waves with dips greater than about 45 degrees have been filtered away by numerical viscosity. The loss of this energy plus the loss of the energy of waves which propagate at complex angles results in a reconstruction (right-hand frame) in which the impulses are somewhat spread out in the horizontal direction.

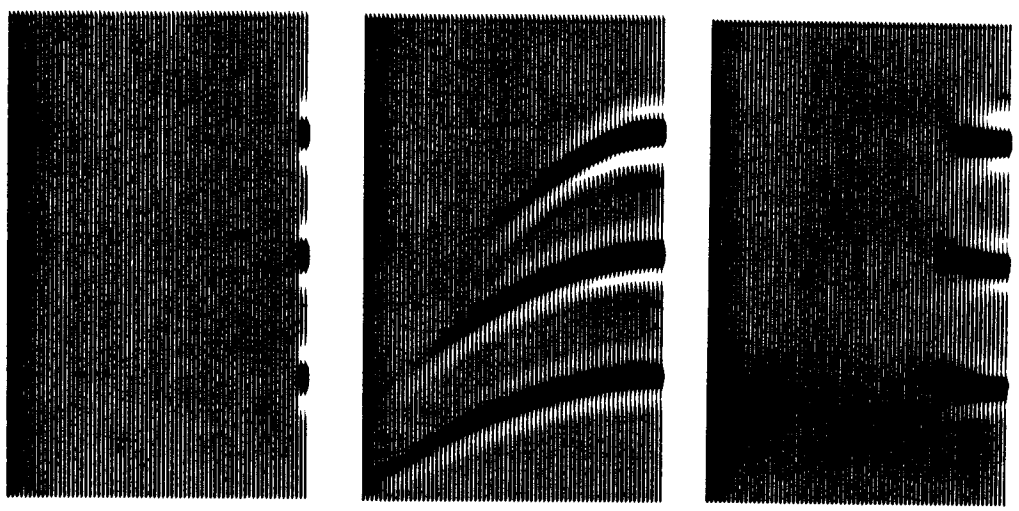

FIG. 8. The time response to depth-domain impulses and reconstruction of the impulses. The left frame depicts a model of the earth which consists of three point scatterers beneath one another along the right-hand edge. The second frame is the synthetic time data created from the model. Basically one observes the hyperbolic traveltime curves to the reflecting points. The third frame represents migration of the synthetic data back to the point scatterers. As in Figure 6 there is a reduced resolution because, in principle, horizontal resolution cannot be better than vertical resolution (which is controlled by the frequency content of the waves) and in practice we have included only rays up to angles of about 40 degrees.

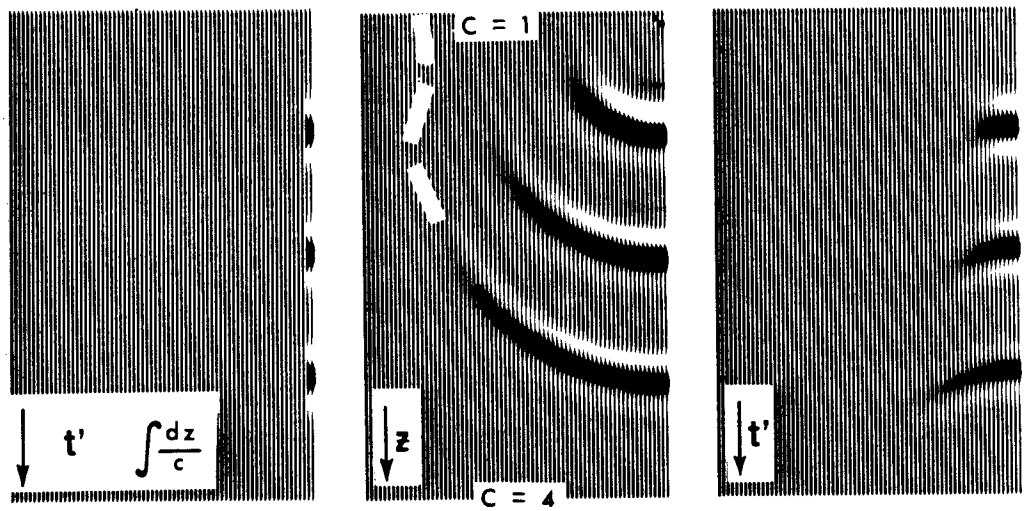

FIG. 9. Response to time-domain impulses in a velocity gradient. The gradient of inverse velocity is constant such that the velocity ranges over a factor of 4 from top to bottom of the frames. The first frame appears like the uniformly spaced (say 1, 2, 3) pulses of Figure 7. However, here the vertical coordinate is not time t but

$$t' = \int c^{-1} dz = \int (az + b) dz.$$

Thus the pulses are really spaced at times proportional to (.9, 1.6, and 2.0). The second frame represents the depth section. The circles of Figure 7 have changed to a narrower shape. If the rays were not cut off around 45 degrees, the shapes would resemble roughly that of a light bulb as indicated by the dashes. The third frame shows the reconstruction of the time data. It clearly deteriorates with depth. This is probably a result of the fact that a 40-degree beam halfwidth at the bottom reflector collapses to a 10-degree beam halfwidth at the surface because of ray curvature. There is also some erroneous bias in the reconstruction (the pulses "bend" a little). This is probably a result of inadequate dip filtering. At the time of writing we are uncertain how much the resolution loss in a velocity gradient results from our method and how much is fundamental.

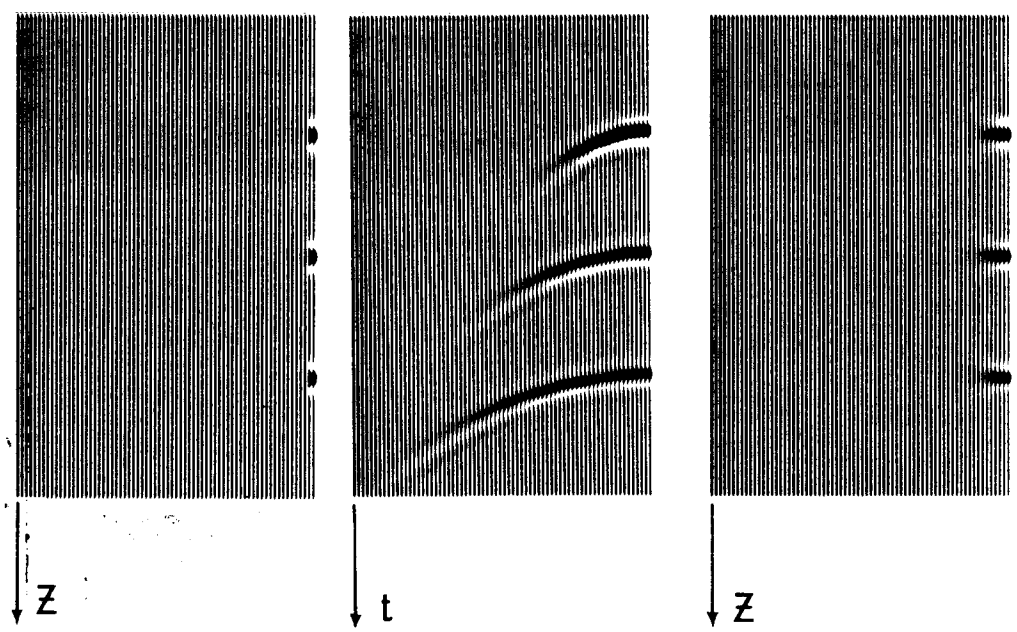

FIG. 10. This is like Figure 8 but the computer grid was not quite fine enough. Note "tails" on the ends of the hyperbolas. The resulting error is explained in the frequency domain in Figure 6. Note that the reconstruction is unaffected. Thus, the ability to reconstruct does not assure a high-quality migration.

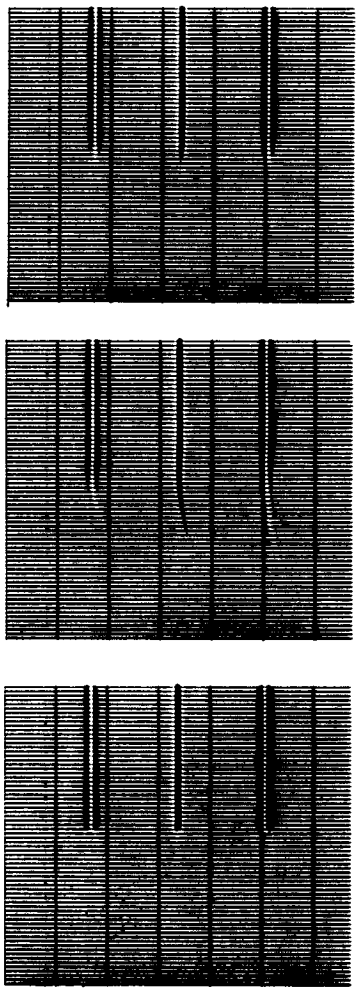

FIG. 11. Acoustic response to terminating interfaces and reconstruction. The left frame illustrates the (x, z) plane with three terminating interfaces. The central frame represents the synthetic "sparker-profile" data $[(x, t)$ plane]. The left branches of the hyperbolas have the polarity of the interface, but the right branches have the opposite polarity. This phenomenon was predicted by Trorey (1970). The rightmost frame is the attempted reconstruction of the model in the first frame.

Differentiating (42) with respect to z' holding x and d fixed, gives

$$t_{z'} = -1/c(z'). \tag{44}$$

Now we can proceed to find d_t and d_z. Substituting (43) into (33) we find

$$d_t = \frac{c(d)}{2}. \tag{45}$$

Substituting (45) and (43) into (34) gives

$$d_z = \frac{c(d)}{2c(z')}. \tag{46}$$

Finally, we may substitute the partial derivatives from (46), (45), and (41) into the downward-continuation equation (26). Substituting (41), (45), and (46) into (26) and omitting $M_{z'z'}$, we get

$$\frac{c(d)}{c(z')} M_{dz'} + M_{xx}\left(\frac{c^d}{2c^d - c^{z'}}\right)^2 + \frac{c(d)^2}{4} \cdot \left(\frac{1}{c(z')^2} - \frac{1}{\bar{c}(x, d, z')^2}\right) M_{dd} = 0. \tag{47}$$

If we assume that the velocity of waves in the earth depends only on depth, then we may take $c(z') = c(x, d, z')$ and (47) reduces to

$$M_{dz'} = -\frac{c(z')}{c(d)}\left(\frac{c^d}{2c^d - c^{z'}}\right)^2 M_{xx}. \tag{48}$$

This equation has the same mathematical form as (9) and the same computer algorithm may be used again.

Equation (48) is limited to rays of moderate angle from the z axis. This equation was used for Figures 11, 13, 14, 18, 19, 20, and 21. In the remaining figures where steeper ray angles were of interest, the M_{zz} term was included by the method of Claerbout (1971a).

SHOT-GEOPHONE OFFSET

If first-order terms in the offset parameter x/d had been retained in the deduction of (27), we would have instead

$$\left(\partial_d + \frac{x}{d}\partial_x\right)\partial_{z'} M = -\left(\frac{d}{2d - z'}\right)^2 \partial_{xx} M. \tag{49}$$

The new term in (49) becomes important if the inequality

$$1 \gg \frac{x}{d}\frac{M_x}{M_d} \tag{50}$$

is not sufficiently strong.

The parameter x/d is a measure of shot-geophone offset. The expression M_x/M_d is the tangent of the local angle of dip. Thus, the new term in (49) is not really necessary if the offset, or the dip, or the product of offset with dip is sufficiently small. Thus, we may expect that the simpler equation without the offset term will be valid for migrating data over a fairly large range of offsets if the dip is not too large. Now consider the occurrence of the symbol x in the coefficient x/d and as an argument of $M(x, d, z')$. On the basis of our derivation, these two x's are the same x. However, since x/d can usually be neglected (i.e., reset to an arbitrary small value), we may regard the x in x/d as independent of the x in $M(x, d, z')$. In $M(x, d, z')$ the argument x refers to the horizontal coordinate (depth point) on the depth profile. In x/d the x refers to the offset of the shot from the depth point. We have shown that this offset is not very important. This is a mathematical justification for stacking moveout-corrected data from many shotpoints before migration in cases where the product of refractor dip and offset is small. Problems may be expected to arise when the dip or offset is great enough. This may correspond to Levin's statement (1971), based on ray geometry, that stacking velocity depends on dip. A procedure (refer to Figure 5) will be described which is intended for use with data which has several offsets or dips (hence several stacking velocities) present in the same region of y and t.

First, moveout-corrected time sections S_0, S_1, S_2, $\cdots$ can be constructed such that S_0 is made up of all data of zero and small offset S_1 is data with a somewhat larger offset, etc. Then the different S_j may be separately migrated through the use of (49) or its generalization to depth-variable velocity. Since the earth itself is invariant to changes in shot-receiver offset, the migrated S_j should also be invariant to offset. Thus, regardless of dip, the migrated S_j should stack without destructive interference. In fact, the velocity which should be used in construction of the S_j is that for which the migrated S_j stack best.

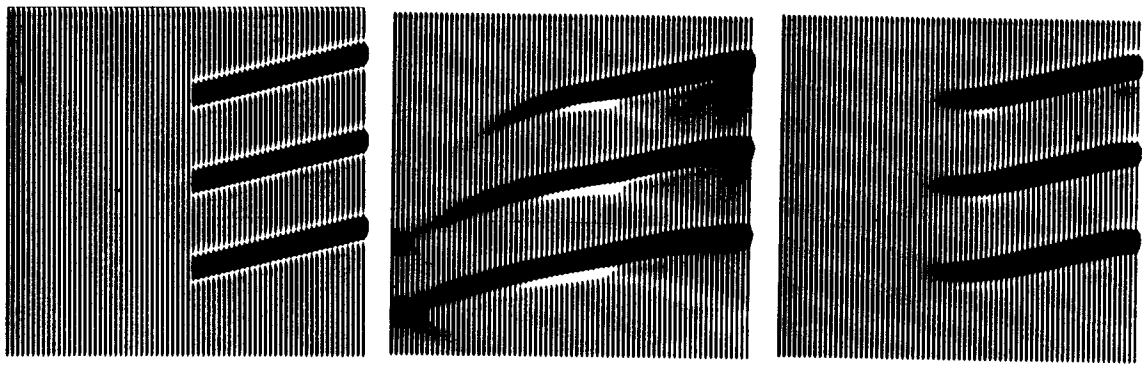

FIG. 12. Like Figure 11 except that the beds have dip. Note that the hyperbolas stay in place but in the time data the interfaces slide down and to the left. (They migrate.) The hyperbolas in the time data would become far more dominant if data were recorded with automatic gain control.

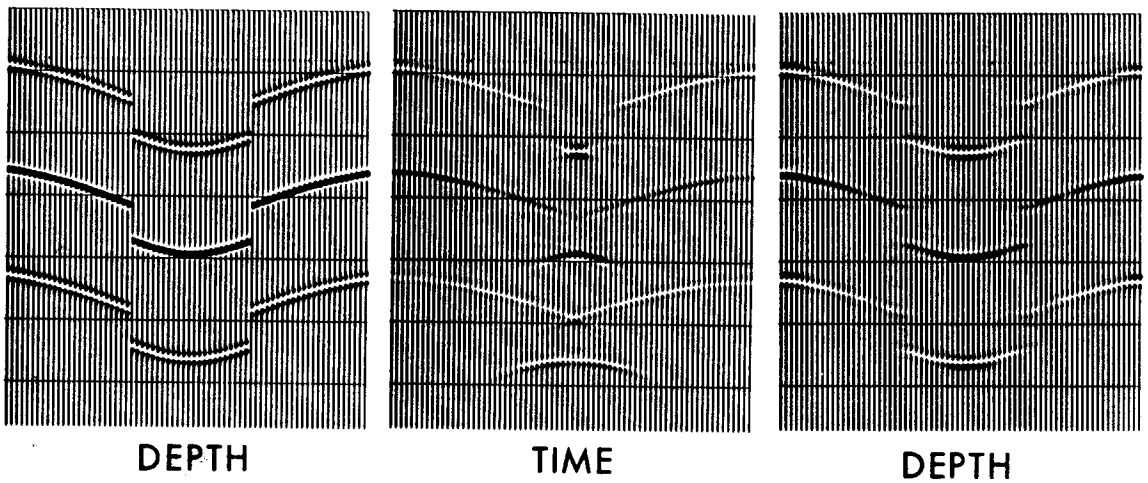

FIG. 13. The classical graben or buried-channel model. Each discontinuity in the depth section gives rise to a faint hyperbola in time.

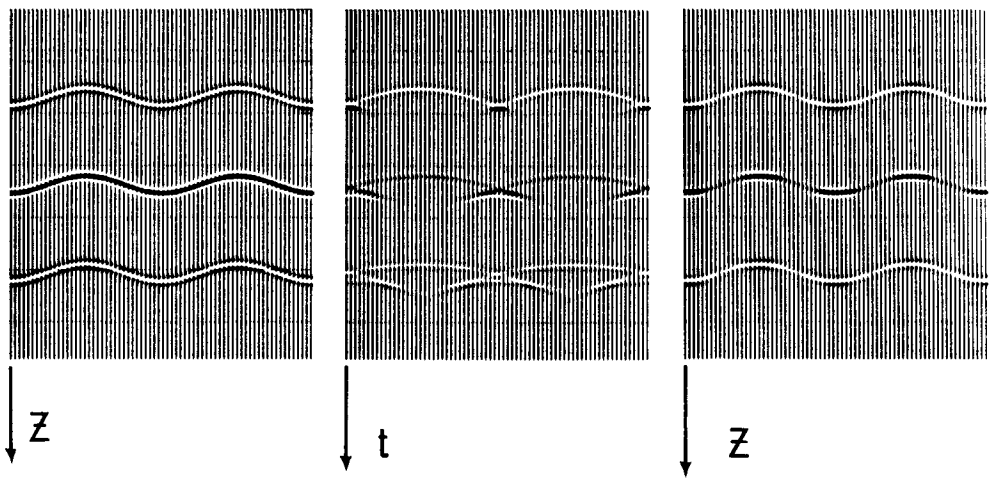

FIG. 14. Sinusoidal interfaces causing many buried foci. Traveltime triplication may be observed readily at the buried foci. Amplitude variations along the reconstructed interfaces arise because dip filtering has been applied on both the data-construction step and the model-reconstruction step.

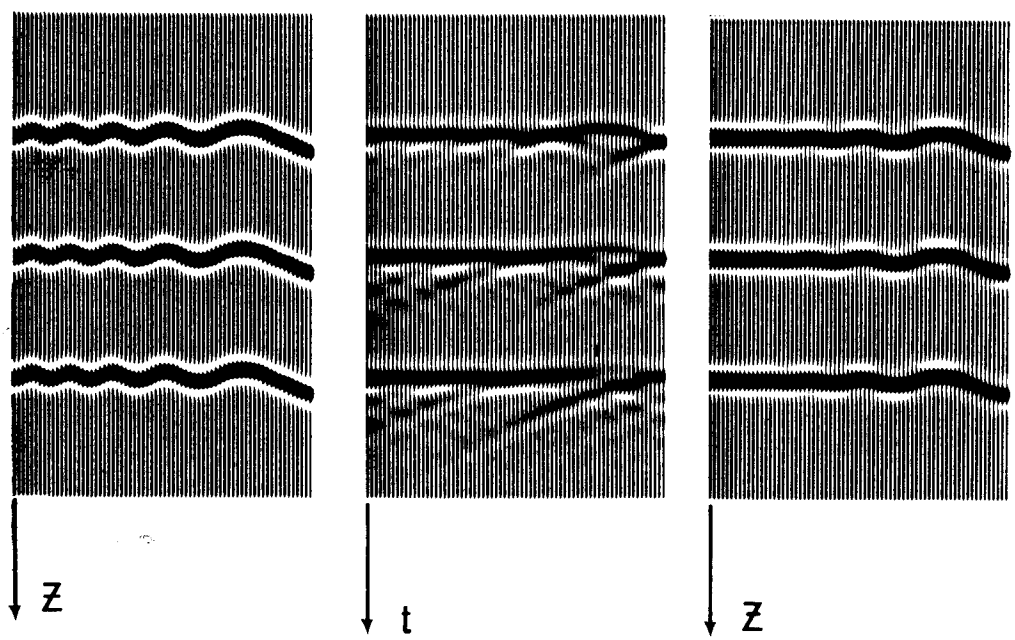

FIG. 15. Undulating interfaces illustrating that horizontal resolution is equal to or less than vertical resolution. A horizontally propagating wave can give as good a horizontal resolution as a vertically propagating wave gives vertical resolution. The dip-filtering operations mentioned in Figure 6 will tend to further degrade horizontal resolution. It will be noted that the rapid oscillations on the left side of the interfaces have not been reconstructed in the rightmost frame.

FIG. 16. The effect of unremoved static errors on migration. The left frame depicts reflections from flat layers plus a static timing error which varies sinusoidally from trace to trace. The result of migration is shown on the right. Note that maxima may be aligned into circular arcs.

FIG. 17. A seismic section across some diapir like structures. This unprocessed data is from the Unmak Plateau in the southeastern Bering Sea (Scholl and Marlow, 1970). The water depth is about a mile. The vertical exaggeration is about 8. This is single-channel, constant offset data. For processing purposes it was considered to be a zero-offset section.

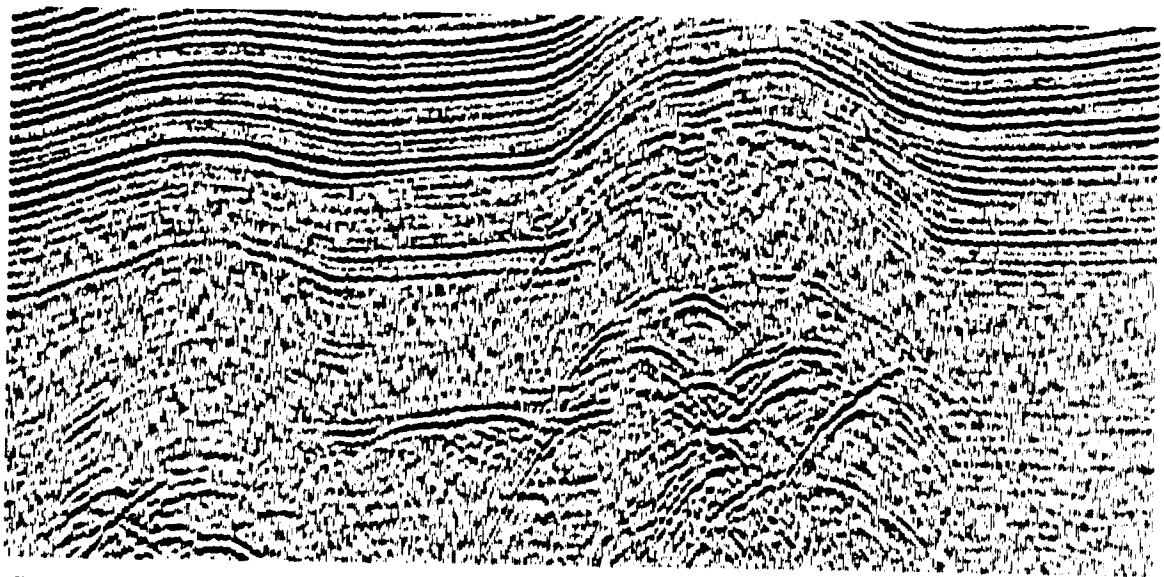

FIG. 18. Enlarged reproduction of the rightmost two domes of Figure 17. Near the top where dips are gentle, the time data may depict a reasonable cross-section of the dome, but the hyperboloids near the bottom arise by scattering from reflecting regions which are considerably smaller than the hyperboloids. Vertical exaggeration is 5.

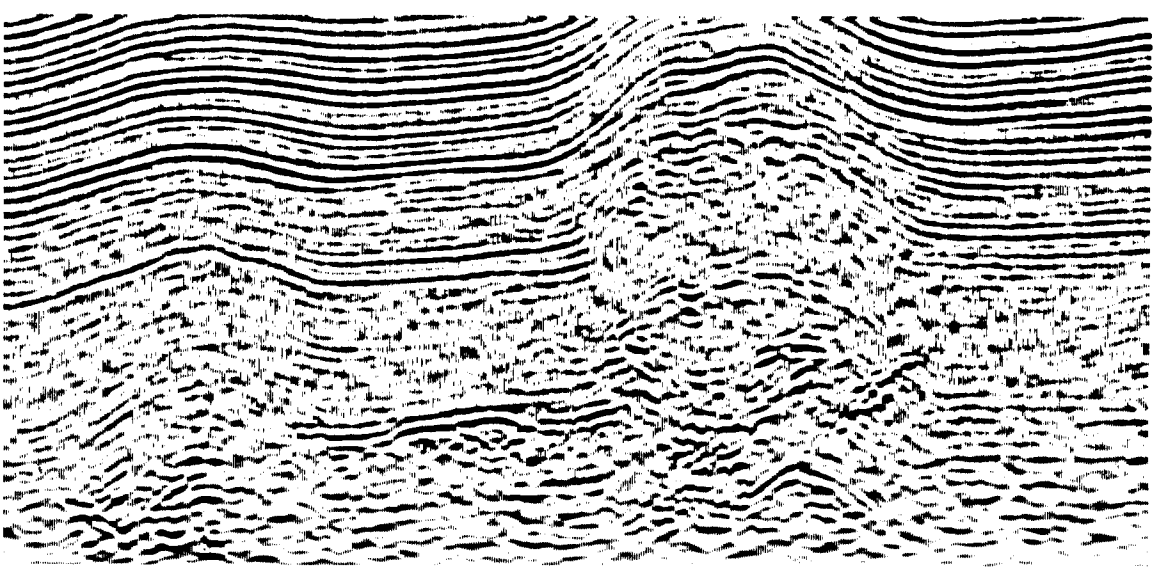

FIG. 19. The first sparker data ever to be migrated by utilizing field data as boundary conditions for a partial-differential equation. These are the data of Figure 18. Hyperbolas have collapsed to smaller scattering centers giving a better picture of the inner part of the dome. Fuzz, due perhaps to sea swell, has disappeared because impossibly steep dips have been attenuated with numerical viscosity. Since all interference effects have not been eliminated (even in the top of the dome) the necessary conclusion is that echoes simultaneously arrive from both sides of the ship. (By the nature of the process, there cannot be simultaneous front-back echoes in the processed data.) Thus, the structure is more complicated than a dome of rotation about the vertical axis. Hence more profiles are required to uniquely delineate the features. The vertical exaggeration is about 5. The data have been processed to dip tangents of about 1/10.

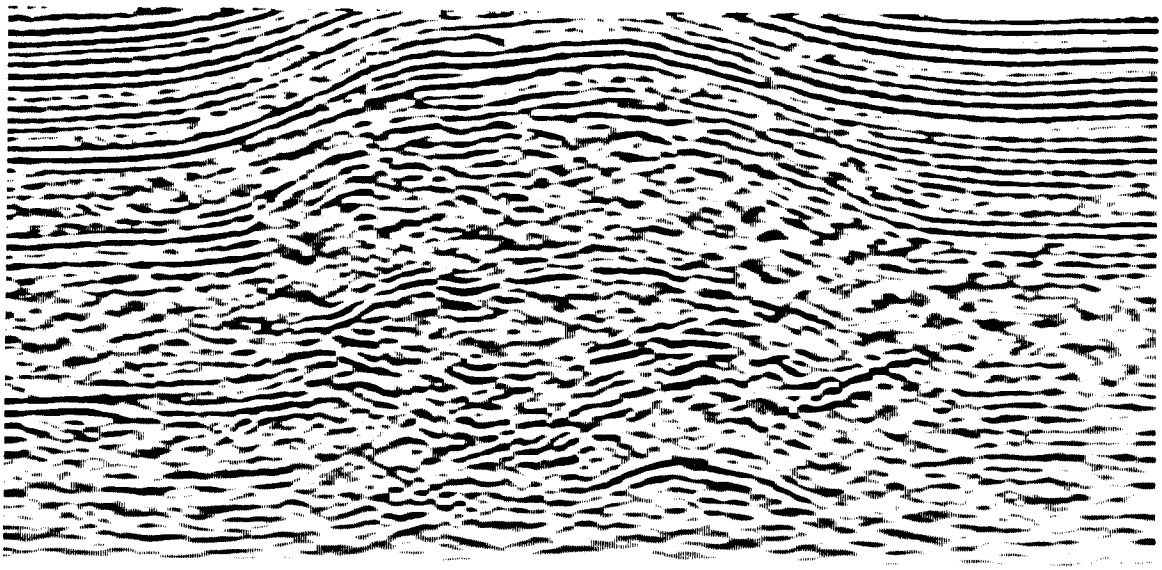

FIG. 20. The rightmost dome of previous figures was further expanded horizontally and processed to dip tangents of about 1/5. Despite the extra processing it is not clear that there has been any improvement over Figure 19. In fact, some circular arcs reminiscent of Figures 7 or 16 are beginning to appear. Such arcs could result from spikes in the data. Actually, we do not believe there are spikes in the data but suspect that these arcs result from some data collection problem as the shipboard AGC changing from channel to channel.

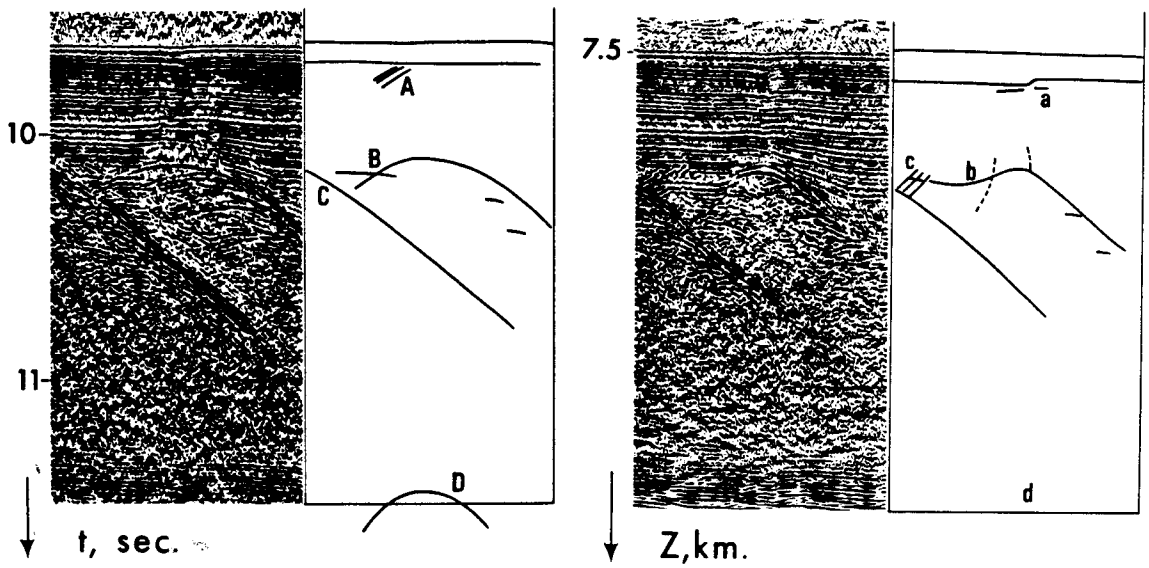

FIG. 21. Migration of Aleutian Trench data. The leftmost frame shows the original data. Note that the top 9 sec, which is the water path, have been omitted. The vertical exaggeration with respect to water velocity is 5.3. Hyperbolic branches at *A* migrate to a small zone *a* where flat-lying sediments are abruptly offset. Traveltime triplication seen at *B* migrates to the concavity at *b* which caused the buried focus. Some undesirable side effects of the process occur around the edges of the frame because of the limited computer memory available. For example the reflector labeled *C* should migrate leftward and upward and partly out of the figure (= the computer memory). In fact, what happens is that a Snell's law of reflection takes place at the side boundary so that the energy appears at *C*. There is also a boundary effect at the bottom of the page. If a hyperbola were to appear as indicated at *D*, its bottom flanks would be cut off by the page boundary. This limits the amount of dip which may be seen at *d*, hence the smoothness in the bottom part of the migrated section.

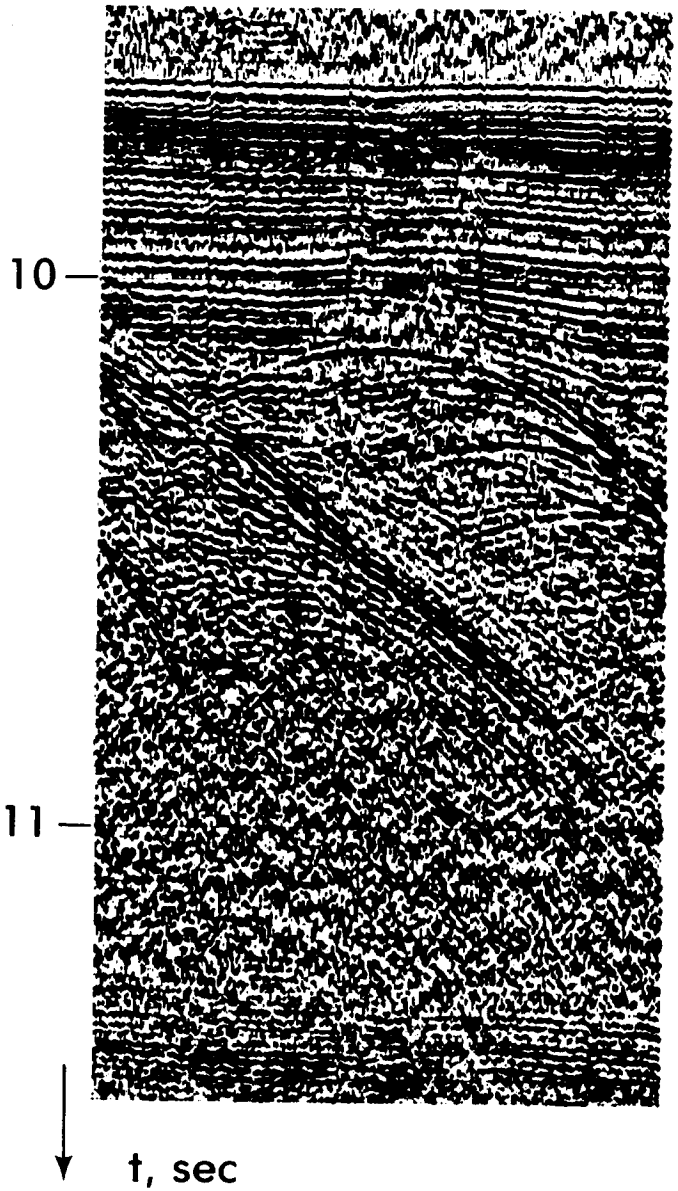

FIG. 22. Enlarged view of the original data shown in Figure 21.

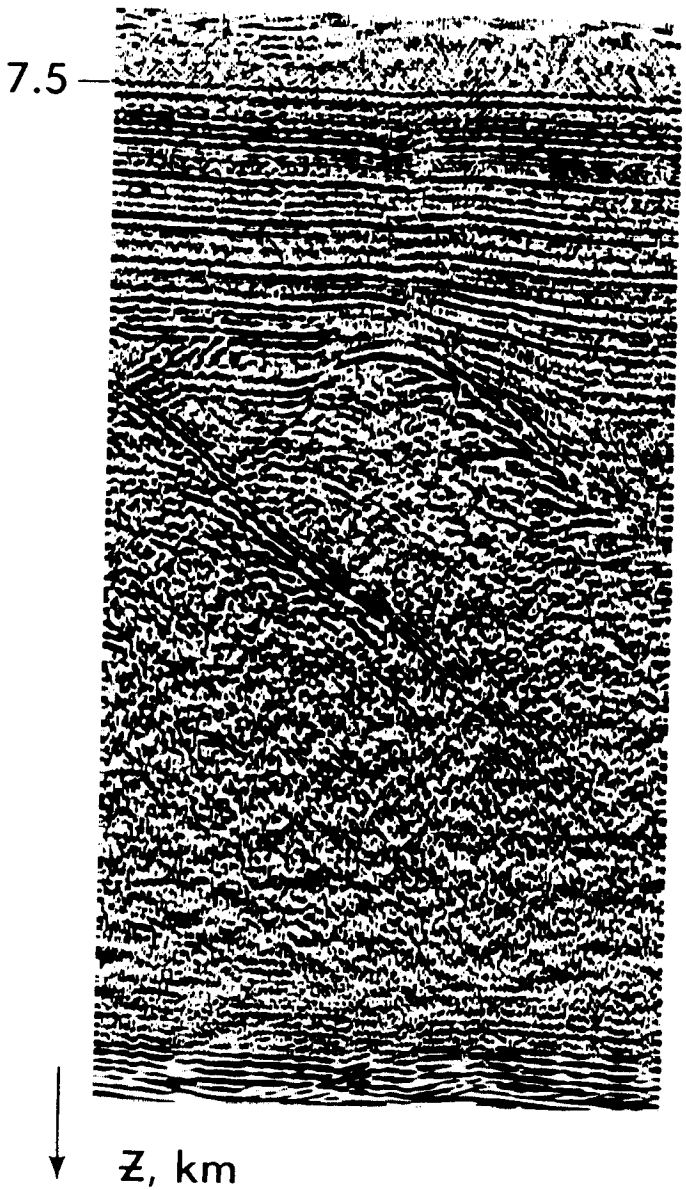

FIG. 23. Enlarged view of the migrated section shown in Figure 21.

This velocity, because it is based on migrated data, should not be subject to the diffraction problem discussed by Dinstel (1971). If the data is "in plane" it should be the true material velocity despite bedding curvature or diffraction.

ACKNOWLEDGMENTS

We wish to express our thanks to the National Science Foundation who supported this work in the early stages, to the donors to the Petroleum Research Fund of the American Chemical Society, and to the Chevron Oil Field Research Company.

REFERENCES

Claerbout, J. F., 1970, Coarse grid calculations of waves in inhomogeneous media with application to delineation of complicated seismic structure: Geophysics, v. 35, no. 3, p. 407–418.

— 1971a, Numerical holography, *in* Acoustical holography, vol. 3: New York, Plenum Press, p. 273–283.

— 1971b, Toward a unified theory of reflector mapping: Geophysics, v. 36, no. 3, p. 467–481.

Claerbout, J. F., and Johnson, A. G., 1971, Extrapolation of time dependent waveforms along their path of propagation: Geophys. J. of the Roy. Astr. Soc., v. 26, no. 1–4, p. 285–294.

Dinstel, W. L., 1971, Velocity spectra and diffraction patterns: Geophysics, v. 36, no. 2, p. 415–417.

Hilterman, F. J., 1970, Three-dimensional seismic modeling: Geophysics, v. 35, no. 6, p. 1020–1037.

Landers, T. E., and Claerbout, J. F., 1972, Elastic waves in laterally inhomogeneous media: J. Geophys. Res., v. 77, p. 1476–1482.

Levin, F. K., 1971, Apparent velocity from dipping interface reflections: Geophysics, v. 36, no. 3, p. 510–516.

Scholl, D. W., and Marlow, M. S., 1970, Diapirlike structures in the southeastern Bering Sea, Bull. AAPG, v. 54, no. 9, p. 1644–1650.

Treitel, S., Shanks, J. L., Frasier, C. W., 1967, Some aspects of fan filtering: Geophysics, v. 32, no. 5, p. 789–800.

Trorey, A. W., 1970, A simple theory for seismic diffractions: Geophysics, v. 35, no. 5, p. 762–784.